Int. J. Heat Mass Transfer. Vol. 30, No. 8, pp. 1733–1741, 1987
Printed in Great Britain

0017–9310/87 $3.00 + 0.00

Performance of air-to-water copper finned-tube heat exchangers at moderately low air-side Reynolds numbers, including effects of baffles

S. A. IDEM, C. JUNG,† G. J. GONZALEZ‡ and V. W. GOLDSCHMIDT
Ray W. Herrick Laboratories, School of Mechanical Engineering, Purdue University, West Lafayette, IN 47907, U.S.A.

(*Received* 30 *April* 1986 *and in final form* 17 *February* 1987)

Abstract—The effects of 'T baffles' upon the performance of a copper finned-tube air-to-water heat exchanger are considered. Basic techniques for quantifying heat exchanger performance are reviewed. Convective heat transfer coefficients are presented as plots of Colburn *j*-factor vs Reynolds number based on hydraulic diameter. Test data are extended to include lower air flow rates than were previously reported in the literature. Friction effects induced by the use of baffles are also examined and presented as plots of friction factor vs Reynolds number.

INTRODUCTION

FINNED-TUBE heat exchangers are encountered in a wide variety of applications, including industrial boilers, commercial warm air furnaces and water heaters, and residential hydronic heaters. This paper provides empirical correlations of experimental heat transfer and flow friction data for air-to-water finned-tube heat exchangers. With these correlations, the performance characteristics of untested but geometrically similar heat exchangers can be predicted, within the parameter range of the correlations.

The performance of copper finned-tube air-to-water and similar heat exchangers has been analyzed by Boot [1], Briggs and Young [2], Gianolo and Cuti [3], Kays and London [4], Legkiy *et al.* [5], Mirkovic [6], Shah [7], and Zukauskas [8], among many others. While various geometries are reported in the literature, the air-side Reynolds number (based on the hydraulic diameter of the flow passage and on the maximum velocity in the passage) for most of the reported data is well above 1000. The test data are now extended to include much lower air flow conditions, spanning Reynolds numbers from 160 to 400 (expected to exhibit essentially laminar flow). This range, in which most appliances operate, has not been reported previously in the literature. Data in the Reynolds number range from 400 to 1600 (expected to exhibit transition to turbulent flow) are also presented.

Baffles placed between adjacent coils may be employed for heat transfer enhancement. Limited test data comparing the performance of baffles were presented in refs. [9, 10]. Those data are now updated and extended through a comparison of the performance of a fin and tube heat exchanger with and without 'T baffles'.

TEST SET-UP AND INSTRUMENTATION

The test coil is a cross-flow heat exchanger with eight helically-fined copper tubes arranged in a single row. The characteristic dimensions are summarized in Table 1. Baffle geometry is presented in Fig. 1, and the flow circuiting is shown in Fig. 2.

The test arrangement is shown in Fig. 3. The horizontal segment of the duct is 10.97 m long, 30.5 cm high and 76.2 cm wide. Two layers of 2.54 cm thick fiberglass insulation shroud the entire wind tunnel, thus reducing heat loss from the system. Air at room temperature is drawn in by the blower (1),§ and then forced through a narrow vertical heating section, where eight electrical resistance heating elements (2) are installed. The small cross-sectional area in this part provides high air velocities and thus enhances heat transfer between the heaters and the air. All eight

Table 1. Characteristic dimensions of the heat exchanger (refer to Fig. 4)

D_i	1.59 cm (0.625 in)
D_o	1.91 cm (0.75 in)
D_f	3.76 cm (1.48 in)
δ	0.053 cm (0.021 in)
S_t	3.89 cm (1.53 in)
A_{tot}	3.45 m^2 (5353 in^2)
A_o	0.232 m^2 (360 in^2)
A_{min}	0.109 m^2 (169 in^2)
σ	0.47
D_H	0.495 cm (0.195 in)
S_f	7 fin in^{-1} (2.7 fin cm^{-1})

† Presently with Brown Boveri-York, Mannheim 1, West Germany.
‡ Presently with CAFESA, San Jose, Costa Rica.
§ Characters in parentheses refer to Fig. 3.

NOMENCLATURE

A	area [m^2 (ft^2)]
C	heat capacity rate [W $°C^{-1}$ (Btu h^{-1} $°F^{-1}$)]
C_r	heat capacity rate ratio, C_{min}/C_{max}
D	diameter [m (ft)]
f	friction factor
G	mass velocity, ρu_{max} [kg m^{-2} s^{-1} (lb_m ft^{-2} s^{-1})]
h	heat transfer coefficient [W m^{-2} $°C^{-1}$ (Btu h^{-1} $°F^{-2}$ $°F^{-1}$)]
H_f	straight fin height [m (ft)]
j	Colburn j-factor, $St\,Pr^{2/3}$
k	fluid thermal conductivity [W m^{-1} $°C^{-1}$ (Btu h^{-1} ft^{-1} $°F^{-1}$)]
k_w	tube wall thermal conductivity [W m^{-1} $°C^{-1}$ (Btu h^{-1} ft^{-1} $°F^{-1}$)]
K_c	entrance pressure loss coefficient
K_e	exit pressure loss coefficient
L	tube length [m (ft)]
L_{eff}	effective heat exchanger length [m (ft)]
$\dot{m}$	mass flow rate [kg s^{-1} (lb_m s^{-1})]
N	number of tubes
Nu	Nusselt number, $h_o D_h/k$
NTU	number of transfer units, $U_o A_{tot}/C_{min}$
P	perimeter [m (ft)]
Pr	Prandtl number, ν/α
Δp	pressure drop [N m^{-2} (lb in^{-2})]
$\dot{Q}$	heat transfer rate, w [Btu h^{-1}]
r	tube radius [m (ft)]
R	thermal resistance [°C W^{-1} (h °F Btu^{-1})]
Re	Reynolds number, $\rho u_{max} D_h/\mu$
S_f	fin pitch [fins m^{-1} (fins ft^{-1})]
S_t	transverse tube pitch [m (ft)]
St	Stanton number, $Nu/Re \cdot Pr$
T	temperature [°C (°F)]
u	fluid velocity [m s^{-1} (ft s^{-1})]
u_o	average velocity across heat exchanger [m s^{-1} (ft s^{-1})]
u_{max}	maximum velocity across heat exchanger [m s^{-1} (ft s^{-1})]
U_o	overall heat transfer coefficient [W m^{-2} $°C^{-1}$ (Btu h^{-1} ft^{-2} $°F^{-1}$)]
v_1	inlet specific volume [kg m^{-3} (lb_m ft^{-3})]
v_2	outlet specific volume [kg m^{-3} (lb_m ft^{-3})]
V_m	average specific volume, $(v_1+v_2)/2$ [kg m^{-3} (lb_m ft^{-3})].

Greek symbols

α	thermal diffusivity [m^2 s^{-1} (ft^2 s^{-1})]
δ	fin thickness [m (ft)]
ε	heat exchanger effectiveness, $\dot{Q}_{act}/\dot{Q}_{max}$
η_f	fin efficiency
η_0	surface efficiency
μ	dynamic viscosity [kg m^{-1} s^{-1} (lb_m ft^{-1} s^{-1})]
ν	kinematic viscosity [m^2 s^{-1} (ft^2 s^{-1})]
ρ	fluid density [kg m^{-3} (lb_m ft^{-3})]
σ	area ratio, $A_{min}A_{fr}$
Σ	summation.

Subscripts

a	air
act	actual
b	bare area
ci	cold fluid inlet
cw	conduction through tube wall
f	fin
fr	frontal
H	hydraulic
hi	hot fluid inlet
ho	hot fluid outlet
i	inside tube
ic	inside convection
max	maximum
min	minimum
o	outside tube
oc	outside convection
s	tube surface
t	total per unit length
tot	total
w	water.

heaters can be switched on and off individually. In addition, the output of the four upper heaters can be individually controlled by means of autotransformers. The maximum output of the elements is 20 kW.

The blower provides a maximum air flow rate in the duct of 40.8 kg min^{-1}. The flow rate can be reduced by closing the damper (3), which is installed downstream of the blower. Further reduction is obtained by opening the bypass window (4), which lets air escape downstream of the damper into the room. Following a diffuser section and a 90° elbow, flow mixers (5) are installed in the horizontal part of the duct, approximately 3.7 m upstream of the heat exchanger. Downstream of the mixers are flow straighteners (6) made of sheets of fibrous material. Two traversing pitot-static tubes (7, 8) are installed in the duct 68.6 cm behind the flow straighteners in orders to obtain the approach velocity distribution. The heat exchanger (9) is 2.0 m downstream of the flow straighteners. This section is insulated with several layers of foam rubber to prevent heat losses to the surroundings. A grid of 20 thermocouples (10), occupying equal duct cross-sectional areas, is installed 0.3 m in front of the heat exchanger to measure the air inlet temperature. Test measurements consistently indicate uniform approach velocity and temperature profiles. Another grid (11)

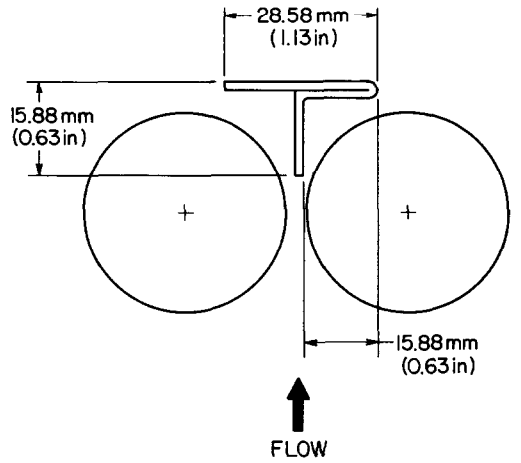

FIG. 1. Baffle geometry.

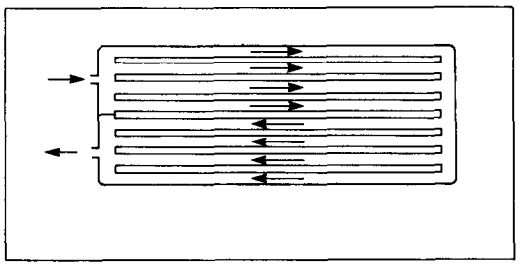

FIG. 2. Heat exchanger flow circuiting.

of the heat exchanger. Perforated diffusion baffles (15, 16) are installed before and after the nozzle section in order to damp out pressure fluctuations. Six thermocouples, occupying equal duct cross-sectional areas, are employed at this location to obtain the temperature for the evaluation of air properties.

The water supply to the heat exchanger is maintained by the 0.60 kW centrifugal pump (17). The water flow rate is measured with a flow meter (18) located downstream of the pump. After passing through the heat exchanger, the water can be directed by means of diverting valve (B) to the main tank (19) or to a smaller weighing tank (20), which is used to calibrate the flow meter. Thermocouples (21) in the main tank monitor the water temperature. If very low flow rates are desired, bypass valve (C) can be opened to ease the load on the pump. The flow rate is controlled by regulating valves (A) and (D).

Water inlet and outlet temperatures are measured at the entrance and exit pipes of the heat exchanger. At both locations the water is well mixed, therefore the bulk water temperature can be measured by means of a single thermocouple (22) which is placed in a well that projects directly into the water stream. All water pipes are insulated with 1.27 cm thick foam rubber insulation.

The mass flow rate of the water is selected to be high enough to provide turbulent flow in the heat exchanger tubes. Hence, the heat transfer resistance is determined mainly by the outside convective heat

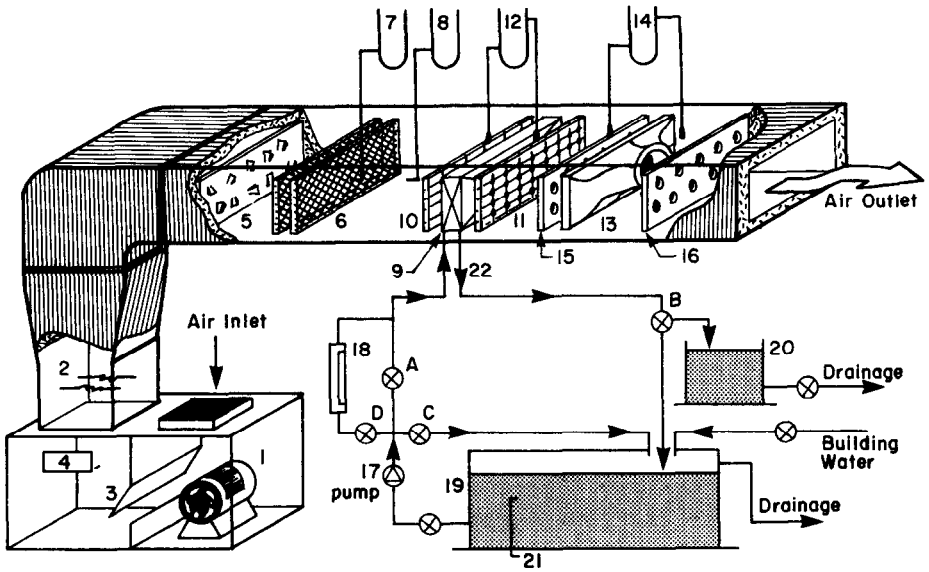

FIG. 3. Wind tunnel test set-up.

with 36 thermocouples, occupying equal duct cross-sectional areas, is situated 0.3 m downstream of the heat exchanger to obtain the outlet temperature. Four static pressure taps (12) located 0.46 m upstream and 1.2192 m downstream of the heat exchanger are used to obtain the pressure drop across the heat exchanger.

A flow nozzle (13) is installed 1.83 m downstream

transfer coefficient. The inside resistance is obtained by means of experimental correlations. Excessive water flow rates are avoided in order that the water temperature rise through the heat exchanger is sufficiently large to measure accurately. A flow rate of 20.4 kg min^{-1} yields satisfactory results.

The inlet temperatures of the air and water, and the

water flow rate through the heat exchanger, are kept constant during all test runs, while the air flow rate is varied from one test to another.

Throughout a run the average air approach temperature is held constant to within $\pm 0.6°C$. The measurement of all temperatures are presumed accurate to within $\pm 0.6°C$. Water flow rates are measured to within $\pm 0.23\,kg\ min^{-1}$, while air-side pressure drops are accurate to within ± 0.025 min of water.

GOVERNING PARAMETERS

The basic dimensionless correlating parameters employed in this experiment are Reynolds number, Nusselt number, Colburn j-factor and the friction factor. These are related by the NTU-effectiveness method, employing the concept of fin efficiency. Some of these parameters are now briefly outlined.

Reynolds number

The Reynolds number, based on the hydraulic diameter and the maximum velocity in the flow passage, can be expressed as

$$Re = \frac{\rho u_{max} D_H}{\mu}. \tag{1}$$

The maximum velocity occurs at the location of the minimum flow area

$$u_{max} = u_o \frac{A_{fr}}{A_{min}} \tag{2}$$

where u_o, the average velocity in the duct, can be defined as

$$u_o = \frac{\dot{m}}{\rho A_{fr}}. \tag{3}$$

Defining σ as A_{min}/A_{fr}, it follows that

$$u_{max} = \frac{\dot{m}}{\rho A_{fr} \sigma}. \tag{4}$$

The hydraulic diameter is generally defined as

$$D_H = 4\frac{A}{P} \tag{5}$$

where P is the perimeter of the duct. For a circular tube D_H is equal to the tube diameter. For the flow passage of non-constant cross-section, D_H can be defined as a ratio of the flooded volume and the total heat transfer area. In this experiment the definition of ref. [4] is used

$$D_H = \frac{4A_{min}L_{eff}}{A_{tot}} \tag{6}$$

where A_{tot} is the total outside heat transfer area of the finned tubes, and L_{eff} is the fin diameter D_f. The Reynolds number can then be evaluated by

$$Re = \frac{4\dot{m}D_f}{\mu A_{tot}}. \tag{7}$$

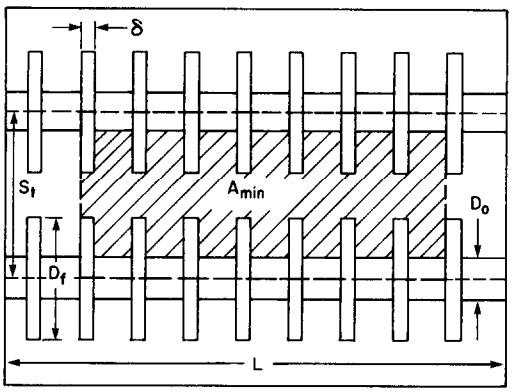

FIG. 4. Heat exchanger characteristic geometry.

With the average fin thickness δ and the fin pitch S_f specified, the total outside heat transfer area per unit length can be calculated as the sum of the area of the bare tube and of the fins

$$A_t = \pi D_0(1-\delta S_f)+0.5\pi S_f(D_f^2-D_o^2)+\pi S_f \delta D_f. \tag{8}$$

For the total heat exchanger surface area

$$A_{tot} = LN\pi[D_o(1-\delta S_f)+S_f(0.5(D_f^2-D_o^2)+\delta D_f)] \tag{9}$$

where D_o is the tube diameter, L the tube length, and N the number of tubes.

The minimum area, A_{min} can be found as

$$A_{min} = NL[(S_t-D_o)-S_f\delta(D_f-D_o)] \tag{10}$$

where S_t is the transverse pitch (see Fig. 4).

Baffles affect the maximum core velocity and the location of the minimum free flow area, and hence the determination of the Reynolds number. The goal of this experiment is to provide a direct comparison between baffled and unbaffled coil surfaces. Thus, it is convenient to base all dimensionless performance correlations on the minimum flow area of the unbaffled geometry.

Colburn j-factor

The Colburn j-factor is defined as

$$j = St\ Pr^{2/3} \tag{11}$$

or, replacing the Stanton number by

$$St = \frac{Nu}{Re\ Pr} \tag{12}$$

it follows that

$$j = \frac{Nu}{Pr^{1/3}\ Re}. \tag{13}$$

Replacing the dimensionless parameters by their definitions

$$Nu = h_o \frac{D_H}{k} \tag{14}$$

$$Re = \frac{u_{max} D_H}{\nu} \tag{15}$$

$$Pr = \frac{\nu}{\alpha} \tag{16}$$

yields

$$j = \frac{h_o \nu}{k u_{max}} (\alpha/\nu)^{1/3} \tag{17}$$

where ν is the kinematic viscosity, α the thermal diffusivity, k the thermal conductivity of the air and h_o is the average outside heat transfer coefficient.

The outside heat transfer coefficient h_o can be determined from the overall heat transfer coefficient, which is defined as

$$U_o = \frac{1}{A_{tot} \Sigma R} \tag{18}$$

based on the outside area A_{tot}. ΣR is the sum of the thermal resistances, which includes the water-side fouling and convective resistance, the air-side fouling and convective resistance, and the conduction resistance through the tube wall. The highest resistance is the convective resistance on the air-side. The fouling resistances are very small and therefore neglected.

The water-side convective resistance can be expressed as

$$R_{ic} = \frac{1}{h_i A_i} \tag{19}$$

with A_i and h_i the inside tube area and heat transfer coefficient, respectively. The latter can be approximated by the Nusselt equation

$$Nu = 0.036 Re^{0.8} Pr^{1/3} (2r_i/L)^{0.055}. \tag{20}$$

The conductive resistance of the wall can be expressed as

$$R_{cw} = \frac{\ln (r_o/r_i)}{2\pi L k_w} \tag{21}$$

with r_i and r_o the inside and outside tube radii, respectively. As the tube area can be expressed as

$$A_i = 2\pi L r_i \tag{22}$$

the resistance can then also be written as

$$R_{cw} = \frac{r_i \ln (r_o/r_i)}{A_i k_w}. \tag{23}$$

The determination of the convective resistance on the air-side must account for the fact that the fin temperature is not constant over the fin length. This is taken into account by the fin efficiency η_f. The heat flow $\dot{Q}_f$ from the fins is given by

$$\dot{Q}_f = h_o A_f \eta_f (T_s - T_a) \tag{24}$$

while the flow $\dot{Q}_b$ from the bare tube can be expressed as

$$\dot{Q}_b = h_o A_b (T_s - T_a) \tag{25}$$

where T_s and T_a are the tube surface temperature and air temperature, respectively, and A_f and A_b the surface areas of the fins and the bare tube. The total heat flow is the sum of that from the fin and bare tube, hence

$$\dot{Q}_{tot} = \dot{Q}_b + \dot{Q}_f = (A_b + \eta_f A_f)/A_{tot} h_o (T_s - T_a) A_{tot}. \tag{26}$$

As $A_b = A_{tot} - A_f$, $\dot{Q}_{tot}$ can also be written as

$$\dot{Q}_{tot} = [1 - A_f/A_{tot}(1 - \eta_f)] A_{tot} h_o (T_s - T_a). \tag{27}$$

The expression in brackets can be redefined as a parameter η_o, the surface efficiency, or

$$\dot{Q}_{tot} = \eta_o A_{tot} h_o (T_s - T_a). \tag{28}$$

The outside convective resistance can then be expressed as

$$R_{oc} = 1/\eta_o A_{tot} h_o. \tag{29}$$

Inserting the above equations into equation (18), and recognizing that

$$\Sigma R = R_{ic} + R_{cw} + R_{oc}$$

yields the following expression for the overall heat transfer coefficient

$$U_o = [A_{tot}/h_i A_i + A_{tot} r_i \ln (r_o/r_i)/A_i k + 1/\eta_o h_o]^{-1}. \tag{30}$$

In order to solve the above equation for h_o the surface efficiency, which is a function of the fin efficiency, must be determined.

Fin efficiency

The amount of heat transferred by convection from the fins to the air is strongly dependent upon the temperature difference between the fin and the air. The maximum heat transfer rate occurs if the fin surface temperature equals the temperature of the tube wall. Due to the conductive resistance of the fin material a temperature gradient occurs along the fin. Thus, the actual amount of heat transferred by convection from the fin is less than the maximum possible. The fin efficiency η_f can be defined as the ratio of the actual heat transfer rate and the above-mentioned maximum rate, i.e.

$$\eta_f = (\dot{Q}_{act}/\dot{Q}_{max})_f. \tag{31}$$

For a straight fin, η_f can be calculated from

$$\eta_f = \tanh (x)/x \quad \text{with} \quad x = H_f (2h_o/k\delta)^{0.5} \tag{32}$$

where H_f is the fin height. For circumferential fins, the relation of ref. [11] can be used, giving an expression for η_f in terms of Bessel functions. Equation (32) can also be applied to circular fins, where the fin height H_f is replaced by a proportional value H_f' [12]

$$H_f' = \left(\frac{D_f}{2} - r_o\right)\left[1 + 0.35 \ln\left(\frac{D_f}{2r_o}\right)\right]. \quad (33)$$

As the fin efficiency is dependent upon the outside convection heat transfer coefficient, it is necessary to calculate h_o iteratively.

NTU-Effectiveness

In order to obtain the overall heat transfer coefficient, the *NTU*-effectiveness method is employed. Consider a counterflow heat exchanger of infinite length. In this case, the fluid with the smaller heat capacity rate C_{min} (where the heat capacity rate C is defined as the product of the mass flow rate and the specific heat) would experience the maximum temperature change. Assuming hot fluid has the minimum capacity rate, for an infinite tube length this fluid would be cooled to the inlet temperature of the cold fluid. Hence the maximum possible heat transfer rate can be defined as

$$\dot{Q}_{max} = C_{min}(T_{hi} - T_{ci}). \quad (34)$$

The actual rate can be obtained from an energy balance

$$\dot{Q}_{act} = C_{min}(T_{hi} - T_{ho}). \quad (35)$$

The effectiveness ε is defined as the ratio of $\dot{Q}_{act}$ and $\dot{Q}_{max}$, i.e.

$$\varepsilon = \dot{Q}_{act}/\dot{Q}_{max} = (T_{hi} - T_{ho})/(T_{hi} - T_{ci}). \quad (36)$$

From this result, the number of transfer units (*NTU*), defined as $(U_o A_{tot}/C_{min})$, can be obtained.

In order to determine a specific form of the ε–*NTU* correlation, an appropriate 'mixing' criteria must be found. A 'mixed' fluid is characterized by a one-dimensional temperature change, while for an unmixed fluid the temperature varies along the normal to the flow direction. Considering an 'unfolded' heat exchanger the water behaves essentially as a 'mixed' fluid with temperature variations only along the flow direction. On the air-side however, temperature variations occur in both directions (along and normal to the direction of the water flow), hence it is unmixed. For this situation [13] the relation

$$\varepsilon = C_r^{-1}\{1 - \exp[-C_r(1 - \exp(-NTU))]\} \quad (37)$$

$$C_r = C_{min}/C_{max} = C_a/C_w \quad (38)$$

$$NTU = \frac{U_o A_{tot}}{C_{min}} = \ln\left\{1 + \frac{C_w}{C_a}\ln\left[1 - \varepsilon\frac{C_a}{C_w}\right]\right\}^{-1}. \quad (39)$$

Thus the overall heat transfer coefficient can be calculated from the experimental data, and h_o, the Nusselt number and the Colburn j-factor can be determined.

Friction factor

Kays and London [4] give the following expression for the pressure drop Δp

$$\Delta p = G^2 v_1/2[(K_c + 1 - \sigma^2) + 2(v_2/v_1 - 1) + fA_{tot}v_m/A_{min}v_1 - (1 - \sigma^2 - K_e)v_2/v_1]. \quad (40)$$

Neglecting the entrance and exit loss coefficients (i.e. $K_c = K_e = 0$), the above equation reduces to

$$\Delta p = G^2 v_1/2[(1 + \sigma^2)(v_2/v_1 - 1) + f(A_{tot}A_{min})(v_m/v_1)]. \quad (41)$$

For small temperature differences the change in the specific volume can be neglected, i.e. $v_1 = v_2$. Then it follows that

$$f = \Delta p 2A_{min}/(u^2 \rho A_{tot}) \quad (42)$$

or, by the definition of the hydraulic diameter

$$f = \Delta p D_H/(2u^2 \rho D_f). \quad (43)$$

TEST RESULTS

Results of tests performed on the baffled and unbaffled heat exchanger over the air-side Reynolds number range 400–1600 are presented in Figs. 5–7. Water mass flow rates of 20.4 kg min^{-1} and air flow rates in excess of 9.1 kg min^{-1} are considered. The j-factors are plotted in Fig. 5. The following correlations are obtained by means of a least-squares curve fit to the data. For the unbaffled heat exchanger

$$j = 0.322Re^{-0.547} \quad (44)$$

whereas with T-baffles

$$j = 0.413Re^{-0.539}. \quad (45)$$

As the plot shows, a considerable increase in heat transfer can be realized by installing baffles. The curves are nearly parallel on the log–log scale. At $Re = 1500$, the j-factor of the unbaffled heat exchanger is 5.90×10^{-3}; the baffles yield a 26.5% increase in j. At lower flow rates, the corresponding increase is lower. For example, at $Re = 500$ the increase in the j-factor is 25.8%. Hence, the baffles exhibit a higher increase in heat transfer for higher air velocities.

Baffles increase the heat transfer rate, mostly due to an increase of the air velocity through the heat exchanger. However, it has to be kept in mind that increasing the velocity improves the heat transfer rate by a power less than one. On the other hand, the pressure drop is dependent on the flow velocity with a power of two or higher. Hence, to get a complete picture of the heat exchanger and baffle performance, the friction factor must be taken into account. Due to the extreme scatter in the experimental value of Δp, it is necessary to fit a least-squares curve to the pressure drop data (not shown) as a function of flow rate. The resulting curve is then incorporated into equation (43) in order to obtain the flow friction correlations displayed in Fig. 6. For the unbaffled heat exchanger

$$f = 0.032Re^{-0.028} \quad (46)$$

whereas with T-baffles

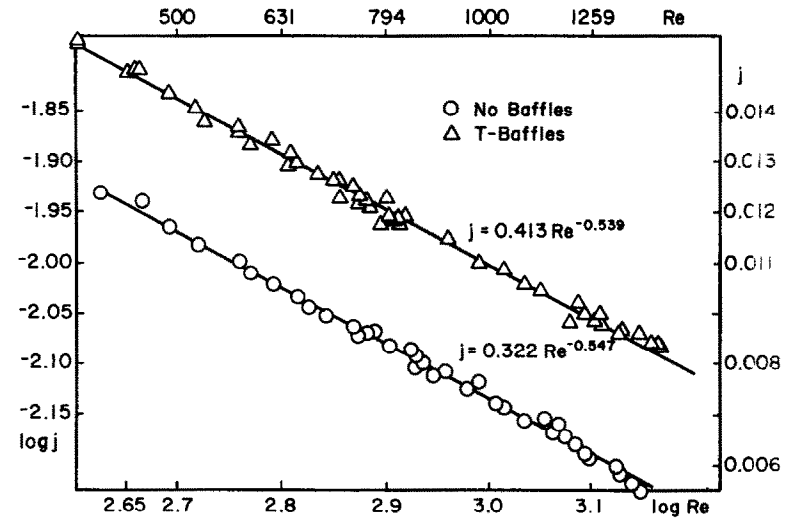

FIG. 5. j-Factors vs Reynolds number.

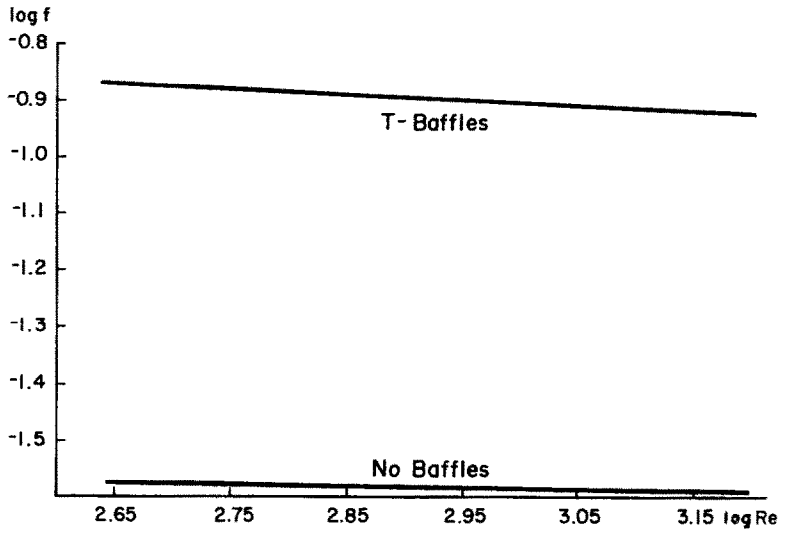

FIG. 6. Friction factor vs Reynolds number.

$$f = 0.238Re^{-0.095}. \quad (47)$$

It can be seen that the T-baffles increase the pressure drop considerably.

The ratio j/f combines heat transfer and friction effects. A 'good' overall performance, i.e. high heat transfer with a low pressure drop, would be indicated by a high value of this ratio. Figure 7 shows plots of log (j/f) vs log Re for the baffled and unbaffled heat exchanger. From this comparison the unbaffled heat exchanger shows higher results and hence best performance. A qualitative trade-off between heat transfer and frictional losses is needed before a final selection is made. This would depend on the specific type of application of the heat exchanger and is not analyzed here.

Tests were also performed on the unbaffled heat exchanger at air flow rates below 9.1 kg min^{-1}, over the Reynolds number range 160–400. The results are plotted in Fig. 8. A least-squares curve fit to the data suggests the following correlation

$$j = 0.391Re^{-0.574} \quad (48)$$

which is very nearly equal to that found for the higher air flow rates.

The trends in the unbaffled heat exchanger data are consistent with those reported in the literature. Kays and London [4] presented j-factors for numerous coil geometries. The j-factor equation slopes ranged from -0.3 to -0.6 for several two pass, staggered, finned-tube heat exchangers operated in overall counter flow. Gonzalez [14] obtained a slope of -0.570 for a nine-tube, staggered configuration, four pass heat exchanger.

CONCLUSIONS

The significant result of this experiment, obtained from the heat exchanger without baffles, is the cor-

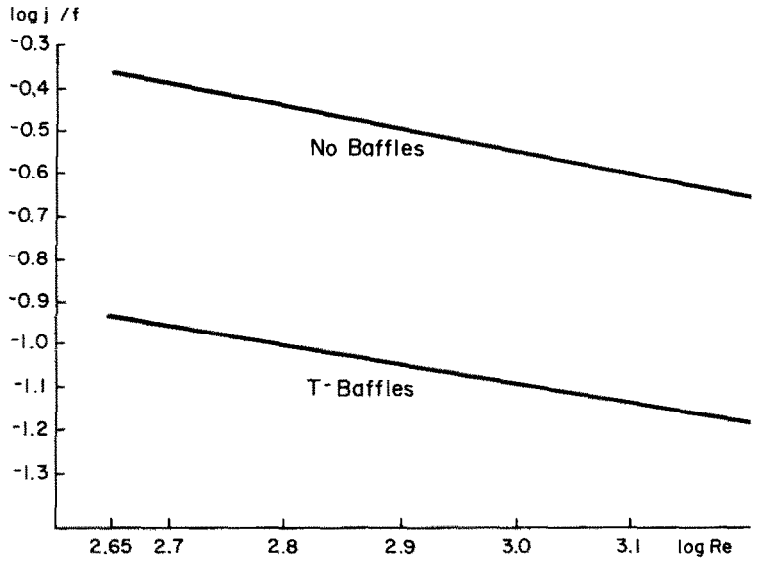

FIG. 7. Heat exchanger overall performance comparison.

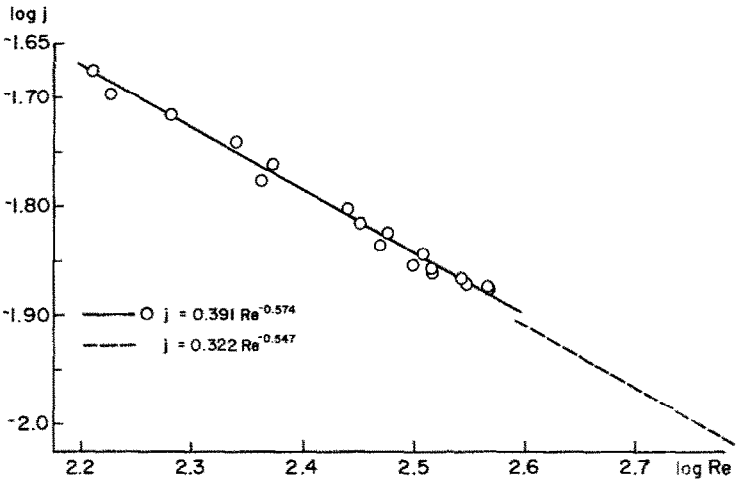

FIG. 8. Low air flow rate Reynolds numbers.

relation for the dimensionless heat transfer parameter

$$j = 0.322Re^{-0.547}. \quad (49)$$

This equation is based on data in a range of air-side Reynolds numbers between 400 and 1600. The tests at lower flow rates, in a Reynolds number range from 160 to 400 yield a similar correlation

$$j = 0.391Re^{-0.574}. \quad (50)$$

Experiments on the heat exchanger with T-baffles attached yield the following correlation

$$j = 0.413Re^{-0.539}. \quad (51)$$

It is found that using baffles augments heat transfer, and hence the j-factor by approximately 26%. Unfortunately, this improvement in heat transfer is accompanied by increases in losses due to pressure drops through the heat exchanger. Further analysis of the relative benefits of both configurations is required.

Acknowledgement—The work presented was part of a research program sponsored by an industrial sponsor. Their support, and excellent technical input through the conduct of the work are acknowledged.

REFERENCES

1. J. L. Boot, Dynamic response model for crossflow heat exchangers, Ph.D. Thesis, Purdue University (1977).
2. D. E. Briggs and E. H. Young, Convection heat transfer and pressure drop of air flowing across triangular pitch banks of finned tubes, *Chem. Engng Prog. Symp. Series No. 41* **59**, 1 (1965).
3. E. Gianolo and F. Cuti, Heat transfer coefficients and pressure drops for air coolers with different numbers of rows under induced and forced draft, *Heat Transfer Engng* **3**(1), 38–48 (July–Sept. 1981).

4. W. M. Kays and M. E. London, *Compact Heat Exchangers*. McGraw-Hill, New York (1984).
5. V. N. Legkiy, V. P. Pavlenko, A. S. Makarov and Y. A. S. Kheludov, Investigation of local heat transfer in a tube with annular fins in transverse air flow, *Heat Transfer—Soviet Res.* **6**(6), 101–107 (Nov.–Dec. 1974).
6. Z. Mirkovic, Heat transfer and flow resistance correlation for helically finned and staggered tube banks in crossflow. In *Heat Exchangers: Design and Theory Sourcebook*, pp. 559–584. McGraw-Hill, New York (1974).
7. R. K. Shah, Compact heat exchangers. In *Heat Exchangers: Thermal–Hydraulic Fundamentals and Design*, pp. 111–151. McGraw-Hill, New York (1981).
8. A. Zukauskas, Air cooled heat exchangers. In *Heat Exchangers: Thermal–Hydraulic Fundamentals and Design*, pp. 49–83. McGraw-Hill, New York (1981).
9. A. W. Lemmon, A. P. Colburn and H. B. Nottage, Heat transfer from a baffled finned cylinder to air, *ASME Trans.* **67**, 601–612 (1945).
10. W. H. McAdams, R. E. Drexel and R. H. Goldey, Local coefficients of heat transfer for air flowing around a finned cylinder, *ASME Trans.* **67**, 613–620 (1945).
11. K. A. Gardner, Efficiency of extended surfaces, *ASME Trans.* **67**, 621 (1945).
12. Th. E. Schmidt, Der Waermeuebergang an Rippenrohren, *Kältetechnik* 4 (1963).
13. F. P. Incropera and D. P. DeWitt, *Fundamentals of Heat Transfer*. Wiley, New York (1981).
14. G. J. Gonzalez, Modeling and testing of a helically finned-tube cross-flow heat exchanger with baffling surfaces, operating at moderately low Reynolds number, M.S. Thesis, Purdue University (1982).

PERFORMANCE DES ECHANGEURS DE CHALEUR AIR–EAU A TUBE AILETE EN CUIVRE, AUX FAIBLES NOMBRES DE REYNOLDS COTE AIR, ET EFFETS DES BAFFLES

Résumé—On considère les effets des baffles en T sur la performance d'un échangeur de chaleur air–eau à tube en cuivre aileté. On passe en revue les façons de quantifier la performance de l'échangeur. On présente des coefficients de transfert thermique sous forme de variation du facteur j de Colburn en fonction du nombre de Reynolds basé sur le diamètre hydraulique. Les données d'essais sont étendues pour inclure les faibles débits d'air. Les effets du frottement induits par l'utilisation des baffles sont aussi examinés et présentés en forme du facteur de frottement fonction du nombre de Reynolds.

WIRKUNGSGRADBESTIMMUNG VON LUFT/WASSER-RIPPENROHRWÄRMEÜBERTRAGERN AUS KUPFER BEI MÄSSIG KLEINEN LUFTSEITIGEN REYNOLDSZAHLEN UNTER BERÜCKSICHTIGUNG DES EINFLUSSES VON UMLENKSCHIKANEN

Zusammenfassung—Es wird der Einfluß von T-förmigen Umlenkschikanen auf den Wirkungsgrad eines Luft/Wasser-Rippenrohrwärmeübertragers aus Kupfer untersucht. Es werden die grundlegenden Bestimmungsmethoden zur Quantifizierung von Wärmetauscherwirkungsgraden überprüft. Der konvektive Wärmeübergangskoeffizient wird in Diagrammen wiedergegeben, in denen der Colburn-j-Faktor über der Reynoldszahl aufgetragen ist. Die Reynoldszahl wird unter Verwendung des hydraulischen Durchmessers ermittelt. Die Testdaten enthalten kleinere Werte für den Luftdurchsatz, als sie bisher in der Literatur zu finden sind. Reibungseffekte, verursacht durch die Umlenkschikanen, werden untersucht und in Diagrammen wiedergegeben, in denen der Reibungsbeiwert über der Reynoldszahl aufgetragen ist.

ЭФФЕКТИВНОСТЬ ТЕПЛООБМЕННИКА ВОЗДУХ-ВОДА ИЗ МЕДНЫХ ОРЕБРЁННЫХ ТРУБ ПРИ ОТНОСИТЕЛЬНО НИЗКИХ ЧИСЛАХ РЕЙНОЛЬДСА ПО ВОЗДУХУ С УЧЁТОМ ВЛИЯНИЯ ПЕРЕГОРОДОК

Аннотация—Рассматривается влияние Т-образных перегородок на эффективность медного оребрённого трубчатого теплообменника воздух-вода. Обсуждается методика оценки эффективности теплообменника. Коэффициенты конвективного теплообмена представлены в виде зависимости j-фактора Колберна от числа Рейнольдса, в котором в качестве характерного размера используется гидравлический диаметр. Опытные данные обобщены для меньших значений расходов воздуха, чем ранее приводившиеся в литературе. Анализируется также сопротивление, вызванное перегородками, которое представлено в виде зависимости коэффициента сопротивления от числа Рейнольдса.